*Inorg. Chem.* **2007**, *46*, 10534–10538


# $\{Ln^{III}[\mu_5\text{-}\kappa^2,\kappa^1,\kappa^1,\kappa^1,\kappa^1\text{-}1,2\text{-}(CO_2)_2C_6H_4][isonicotine][H_2O]\}_2Cu^I\cdot X$ (Ln = Eu, Sm, Nd; X = $ClO_4^-$, $Cl^-$): A New Pillared-Layer Approach to Heterobimetallic 3d–4f 3D-Network Solids

**Jian-Wen Cheng,[†] Shou-Tian Zheng,[†] En Ma,[†] and Guo-Yu Yang*[,†,‡]**

*State Key Laboratory of Structural Chemistry, Fujian Institute of Research on the Structure of Matter, and Graduate School of the Chinese Academy of Sciences, Fuzhou, Fujian 350002, China, and State Key Laboratory of Rare Earth Materials and Applications, Peking University, Beijing 100871, China*

Received May 9, 2007

A new series of heterometallic lanthanide(III)–copper(I) coordination polymers $Ln_2(bdc)_2(ina)_2(H_2O)_2Cu\cdot X$ (Hina = isonicotinic acid; $H_2bdc$ = 1,2-benzenedicarboxylic acid; Ln = Eu (**1**), Sm (**2**), Nd (**3**), X = $ClO_4^-$; Ln = Nd (**4**), X = $Cl^-$) have been hydrothermally synthesized in the presence/absence of $HClO_4$. Both compounds are isostructural and contained two distinct units of 2D Ln–bdc layers and linear $[Cu(ina)_2]^-$. The linear $[Cu(ina)_2]^-$ complexes act as pillars and further link the Ln–bdc layers resulting in four heterometallic metal–organic frameworks, which represent the first pillared-layer 3d–4f framework with two distinct types of channels along the *b* and *c* axes. The compounds can be specified by the Schläfli symbol $(4^7\cdot6^3)(4^7\cdot6^8)$ as a novel 3D (5,6)-connected net. Furthermore, the IR, TGA, PXRD, and UV–vis spectral and luminescent properties of **1**–**4** were also studied.

## Introduction

The design and synthesis of three-dimensional (3D) metal−organic frameworks (MOFs) with porous structures are currently of great interest due to their potential applications in ion exchange, gas storage and separation, nonlinear optics, magnetism, and catalysis.[1] However, most work so far has focused on the assembly of the homometallic porous MOFs,[1,2] while the analogous chemistry and synthetic strategy of 3d−4f heterometallic porous MOFs is still less developed.[3] The competitive reactions between 3d and 4f metals chelated to the same ligand often result in homometallic complexes rather than heterometallic ones. In comparison with a number of homometallic porous and 3d−4f heterometallic nonporous complexes,[1,2,4] only several examples of 3D 3d−4f heterometallic porous MOFs have been reported.[3]

Various approaches have been developed to create MOFs with well-defined pores. Among the reported porous frameworks, pillared-layer assemblies have been proven to be an

* To whom correspondence should be addressed. E-mail: ygy@fjirsm.ac.cn. Fax: (+86) 591-8371-0051.
[†] Chinese Academy of Sciences.
[‡] Peking University.

(1) Recent reviews on porous metal−organic frameworks: (a) Ockwig, N. W.; Delgado-Friedrichs, O.; O'Keeffe, M.; Yaghi, O. M. *Acc. Chem. Res.* **2005**, *38*, 176. (b) Férey, G.; Mellot-Draznieks, C.; Serre, C.; Millange, F. *Acc. Chem. Res.* **2005**, *38*, 217. (c) Hill, R. J.; Long, D. L.; Champness, N. R.; Hubberstey, P.; Schröder, M. *Acc. Chem. Res.* **2005**, *38*, 335. (d) Kitagawa, S.; Kitaura, R.; Noro, S. I. *Angew. Chem., Int. Ed.* **2004**, *43*, 2334. (e) Rao, C. N. R.; Natarajan, S.; Vaidhyanathan, R. *Angew. Chem., Int. Ed.* **2004**, *43*, 1466. (f) Bradshaw, D.; Claridge, J. B.; Cussen, E. J.; Prior, T. J.; Rosseinsky, M. J. *Acc. Chem. Res.* **2005**, *38*, 273. (g) Yaghi, O. M.; O'Keeffe, M.; Ockwig, N. W.; Chae, H. K.; Eddaoudi, M.; Kim, J. *Nature.* **2003**, *423*, 705. (h) James, S. L. *Chem. Soc. Rev.* **2003**, *32*, 276. (i) Rowsell, J. L. C.; Yaghi, O. M. *Angew. Chem., Int. Ed.* **2005**, *44*, 4670. (j) Janiak, C. *J. Chem. Soc., Dalton Trans.* **2003**, 2781. (k) Goldberg, I. *Chem. Commun.* **2005**, 1243. (l) Special issue of *J. Solid State Chem.* **2005**, *178*, 2409−2573.

(2) (a) Zhang, L.; Gu, W.; Li, B.; Liu, X.; Liao, D. *Inorg. Chem.* **2007**, *46*, 622. (b) Pan, L.; Woodlock, E. B.; Wang, X.; Zheng, C. *Inorg. Chem.* **2000**, *39*, 4174. (c) Zheng, X.; Sun, C.; Lu, S.; Liao, F.; Gao, S.; Jin, L. *Eur. J. Inorg. Chem.* **2004**, 3262.

(3) (a) Zhao, B.; Cheng, P.; Dai, Y.; Cheng, C.; Liao, D.; Yan, S.; Jiang, Z.; Wang, G. *Angew. Chem., Int. Ed.* **2003**, *42*, 934. (b) Zhao, B.; Cheng, P.; Chen, X.; Cheng, C.; Shi, W.; Liao, D.; Yan, S.; Jiang, Z. *J. Am. Chem. Soc.* **2004**, *126*, 3012. (c) Ren, Y.; Long, L.; Mao, B. W.; Yuan, Y.; Huang, R.; Zheng, L. *Angew. Chem., Int. Ed.* **2003**, *42*, 532. (d) Baggio, R.; Garland, M. T.; Moreno, Y.; Peña, O.; Perec, M.; Spodine, E. *J. Chem. Soc., Dalton Trans.* **2000**, 2061. (e) Guillou, O.; Daiguebonne, C.; Camara, M.; Kerbellec, N. *Inorg. Chem.* **2006**, *45*, 8468.

(4) (a) Zaleski, C. M.; Depperman, E. C.; Kampf, J. W.; Kirk, M. L.; Pecoraro, V. L. *Inorg. Chem.* **2006**, *45*, 10022. (b) Costes, J.-P.; Shova, S.; Juanc, J. M. C.; Suet, N. *J. Chem. Soc., Dalton Trans.* **2005**, 2830. (c) Gheorghe, R.; Andruh, M.; Costes, J.-P.; Donnadieub, B. *Chem. Commun.* **2003**, 2778. (d) Kou, H.; Zhou, B.; Gao, S.; Wang, R. *Angew. Chem., Int. Ed.* **2003**, *42*, 3288.



10.1021/ic700893w CCC: $37.00 
Published on Web 11/09/2007

effective and controllable route to design 3D frameworks with large and functionalized channels through modification of the pillar fragment in the adjacent layers.[5] To date, organic ligands,[6] simple inorganic ions,[7] polyoxometalates,[8] and coordinated cations via coordination bonding[9a] or hydrogen bonding[9b] have been well-documented to act as pillars in homometallic pillared-layer porous frameworks. A case where the coordinated transition-metal (TM) anions act as pillars that further link the lanthanide−organic layers into a 3D pillared-layer porous 3d−4f framework via coordination bonding has not been reported.

Recently, we initiated a synthetic attempt for making pillared-layer porous 3d−4f complexes. Our synthetic strategy was to make porous 3d−4f MOFs via linking lanthanide−organic layers with coordinated TM pillars on the basis of rational design. 1,2-benzenedicarboxylic acid ($H_2$-bdc) and isonicotinic acid (Hina) have been chosen as the multifunctional bridging ligand based on the following considerations: (1) $H_2$bdc has versatile coordination modes which favor it to form different two-dimensional (2D) nets with lanthanide contraction;[10a] (2) Hina is a rigid ligand with the oxygen atoms preferring to coordinate to Ln ions, while the nitrogen atoms have a strong tendency to coordinate to TM ions, enabling the Hina ligands to act as a linear bridge.[10b] The recognition between lanthanide−organic layers and coordinated TM pillars can effectively prevent lattice interpenetration, which is the most difficult problem encountered in making porous 3d−4f MOFs. The application of an analogous synthetic strategy to pillared-layer mixed TM porous structures was previously reported.[11] Herein, we report four pillared-layer 3d−4f heterometallic coordination polymers: $Ln_2(bdc)_2(ina)_2(H_2O)_2Cu{\cdot}X$ (Ln = Eu (**1**), Sm (**2**), Nd (**3**), X = $ClO_4^-$; Ln = Nd (**4**), X = $Cl^-$) in which the linear $[Cu(ina)_2]^-$ complexes act as pillars and link the lanthanide−organic layers, resulting in pillared-layer 3d−4f mixed-metal frameworks. Although considerable progress has been made in the synthesis of 3D 3d−4f porous nanotubular coordination polymers by using multidentate ligands such as pyridine-2,6-dicarboxylic acid,[3a,b] iminodiacetic acid,[3c] 2,2′-oxydiacetato acid,[3d] and propylenebis(oxamato),[3e] the construction of pillared-layer 3d−4f heterometallic architecture here is significantly different from that of the above nanotubular structures, which provide the first 3d−4f pillared-layer materials with different types of channels.

## Experimental Section

**Materials and Methods.** All chemicals were purchased commercially and used without further purification. Elemental analyses for C, H, and N were performed on a Vario EL III elemental analyzer. The FT-IR spectra (KBr pellets) were recorded on an ABB Bomen MB 102 spectrometer, and the UV−vis spectra were recorded on a Lambda 900 spectrophotometer. Thermogravimetric analysis (TGA) was performed on a Mettler TGA/SDTA 851e analyzer with a heating rate of 10 °C/min under an air atmosphere. Photoluminescence analyses were performed on an Edinburgh Instrument F920 fluorescence spectrometer. Powder X-ray diffraction (PXRD) data were obtained using a Philips X'Pert-MPD diffractometer with Cu Kα radiation ($\lambda$ = 1.54056 Å).

**$Eu_2(bdc)_2(ina)_2(H_2O)_2Cu{\cdot}ClO_4$ (1).** A mixture of $Eu_2O_3$ (0.5 mmol, 0.178 g), Hina (2 mmol, 0.246 g), $H_2$bdc (1.0 mmol, 0.149 g), $CuCl_2{\cdot}2H_2O$ (0.2 mmol, 0.034 g), $H_2O$ (10 mL), and $HClO_4$ (0.7 mmol) was sealed in a 30 mL Teflon-lined bomb and heated at 170 °C for 7 days and then slowly cooled to room temperature. Yellow prismatic crystals of **1** were obtained in 36% yield based on Cu. Anal. Calcd for **1**, $C_{28}H_{20}ClCuEu_2N_2O_{18}$: C, 31.27; H, 1.87; N, 2.61. Found: C, 31.06; H, 2.03; N, 2.70. Energy-dispersive spectrometry (EDS) gives the Cu/Cl/Eu molar ratio in **1** as 1:1.2:2 (calcd Cu/Cl/Eu = 1:1:2). IR bands ($cm^{-1}$) for **1**: 3449(vs), 1588(s), 1566(m), 1509(m), 1435 (m), 1397(m), 1089(s), 763(s), 695(s).

**$Sm_2(bdc)_2(ina)_2(H_2O)_2Cu{\cdot}ClO_4$ (2).** Compound **2** was made by a procedure similar to that of **1**, except $Sm_2O_3$ (0.175 g) replaced $Eu_2O_3$. Yellow prismatic crystals of **2** were obtained in 30% yield based on Cu. Anal. Calcd for **2**, $C_{28}H_{20}ClCuSm_2N_2O_{18}$: C, 31.37; H, 1.89; N, 2.61. Found: C, 31.13; H, 2.68; N, 2.85. EDS gives the Cu/Cl/Eu molar ratio in **2** as 1:1.2:2 (calcd Cu/Cl/Eu = 1:1:2). IR bands ($cm^{-1}$) for **2**: 3447(vs), 1587(s), 1563(m), 1506(m), 1435(m), 1397(m), 1090(s), 763(s), 695(s).

**$Nd_2(bdc)_2(ina)_2(H_2O)_2Cu{\cdot}X$ (X = $ClO_4^-$ (3), $Cl^-$ (4)).** Compounds **3** and **4** were made by a procedure similar to that of **1**, except $Nd_2O_3$ (0.175 g) replaced $Eu_2O_3$. Yellow prismatic crystals of **3** and **4** were obtained in 32 and 15% yield based on Cu with poor quality. X-ray diffraction data on single crystals show that the unit cell is very similar to **1** and **2**. For **3**: monoclinic, space group *C*2, $a$ = 36.935 (5) Å, $b$ = 7.0464(7) Å, $c$ = 6.2156(7) Å, $\beta$ = 97.156(6)°, and $V$ = 1605.1(3) $Å^3$. For **4**: monoclinic, space group *C*2, $a$ = 36.951(4) Å, $b$ = 7.0580(6) Å, $c$ = 6.2155(8) Å, $\beta$ = 97.505 (7)°, and $V$ = 1607.1(3) $Å^3$. The experimental PXRD patterns of **3** and **4** correspond well with the simulated and experimental PXRD patterns of **1** and **2**, further indicating that these compounds are isostructural (Figure 1). Anal. Calcd for **3**, $C_{28}H_{20}ClCuNd_2N_2O_{18}$: C, 31.73; H, 1.90; N, 2.64. Found: C, 31.57; H, 2.37; N, 2.53. IR bands ($cm^{-1}$) for **3**: 3452(vs), 1586(s), 1562(m), 1505(m), 1434(m), 1397(m), 1089(s), 762(s), 695(s). Anal. Calcd for **4**, $C_{28}H_{20}ClCuNd_2N_2O_{14}$: C, 33.77; H, 2.02; N, 2.81. Found: C, 33.30; H, 2.50; N, 2.37. IR bands ($cm^{-1}$) for **4**: 3443(vs), 1585(m), 1558(s), 1505(m), 1435(m), 1396(m), 762(s), 695(s).

**Single-Crystal Structure Determination.** The intensity data were collected on a Mercury CCD diffractometer with graphite-monochromated Mo Kα radiation ($\lambda$ = 0.71073 Å) at room


(5) (a) Kitagawa, S.; Uemura, K. *Chem. Soc. Rev.* **2005**, *34*, 109. (b) Kitaura, R.; Kitagawa, S.; Kubota, Y.; Kobayashi, T. C.; Kindo, K.; Mita, Y.; Matsuo, A.; Kobayashi, M.; Chang, H. C.; Ozawa, T. C.; Suzuki, M.; Sakata, M.; Takata, M. *Science.* **2002**, *298*, 2358. (c) Wang, X.; Qin, C.; Wang, E.; Li, Y.; Hu, C.; Xu, L. *Chem. Commun.* **2004**, 378.

(6) (a) Kitaura, R.; Fujimoto, K.; Noro, S.; Kondo, M.; Kitagawa, S. *Angew. Chem., Int. Ed.* **2002**, *41*, 133. (b) Maji, T. K.; Uemura, K.; Chang, H. C.; Matsuda, R.; Kitagawa, S. *Angew. Chem., Int. Ed.* **2004**, *43*, 3269. (c) Chun, H.; Dyunuk, D.; Kim, K. *Chem.—Eur. J.* **2005**, *11*, 3521. (d) Ma, B.; Mulfort, K. L.; Hupp, J. T. *Inorg. Chem.* **2005**, *44*, 4912. (e) Park, H.; Britten, J. F.; Mueller, U.; Lee, J. Y.; Li, J.; Parise, J. B. *Chem. Mater.* **2007**, *19*, 1302.

(7) (a) Noro, S. I.; Kitagawa, S.; Kondo, M.; Seki, K. *Angew. Chem., Int. Ed.* **2000**, *39*, 2082. (b) Chakrabarti, S.; Natarajian, S. *J. Chem. Soc., Dalton Trans.* **2002**, 4156.

(8) Lü, J.; Shen, E.; Li, Y.; Xiao, D.; Wang, E.; Xu, L. *Cryst. Growth Des.* **2005**, *5*, 65.

(9) (a) Liu, B.; Xu, L. *Inorg. Chem. Commun.* **2006**, *9*, 364. (b) Ding, B. B.; Weng, Y.; Mao, Z.; Lam, C. K.; Chen, X.; Ye, B. *Inorg. Chem.* **2005**, *44*, 8836.

(10) (a) Wan, Y.; Jin, L.; Wang, K.; Zhang, L.; Zheng, X.; Lu, S. *New J. Chem.* **2002**, *26*, 1590. (b) Zhang, M.-B.; Zhang, J.; Zheng, S.-T.; Yang, G.-Y. *Angew. Chem., Int. Ed.* **2005**, *44*, 1385.

(11) Maggard, P. A.; Yan, B.; Luo, J. *Angew. Chem., Int. Ed.* **2005**, *44*, 2553.

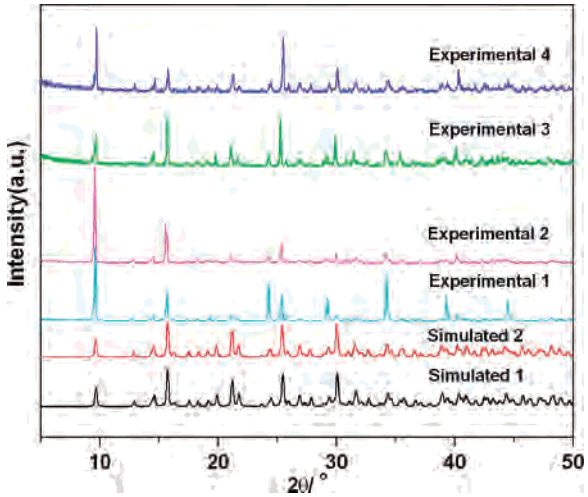


**Figure 1.** Simulated PXRD patterns of **1** and **2** and experimental PXRD patterns of **1**−**4**. The experimental PXRD patterns of **3** and **4** correspond well with the simulated and experimental PXRD patterns of **1** and **2**, indicating that these complexes are isostructural. The difference in reflection intensities between the simulated and experimental patterns was due to the variation in preferred orientation of the powder sample during the collection of the experimental PXRD data.

**Table 1.** Crystal Data and Structure Refinement for Compounds **1** and **2**

| | **1** | **2** |
|---|---|---|
| formula | $C_{28}H_{20}ClCuEu_2N_2O_{18}$ | $C_{28}H_{20}ClCuSm_2N_2O_{18}$ |
| $M_r$ | 1075.37 | 1072.15 |
| cryst syst | monoclinic | monoclinic |
| space group | *C*2 | *C*2 |
| *a* (Å) | 36.860(5) | 36.936(4) |
| *b* (Å) | 6.9900(7) | 7.0081(6) |
| *c* (Å) | 6.2100(7) | 6.2127(7) |
| α (deg) | 90.00 | 90.00 |
| *β* (deg) | 97.020(6) | 97.246(6) |
| *γ* (deg) | 90.00 | 90.00 |
| *V* (Å$^3$) | 1588.0(3) | 1595.3(3) |
| Z | 2 | 2 |
| $D_c$ (g cm$^{-3}$) | 2.249 | 2.232 |
| *μ* (mm$^{-1}$) | 4.738 | 4.465 |
| *F*(000) | 1036 | 1032 |
| GOF | 1.095 | 1.061 |
| collected reflns | 6137 | 6161 |
| unique reflns ($R_{int}$) | 3303 (0.0247) | 3535 (0.0299) |
| observed reflns [$I > 2\sigma(I)$] | 3130 | 3294 |
| refined params | 231 | 231 |
| $R_1{}^a/R_2{}^b$ [$I > 2\sigma(I)$] | 0.0293/0.0698 | 0.0332/0.0811 |
| $R_1{}^a/R_2{}^b$ (all data) | 0.0315/0.0719 | 0.0360/0.0833 |

$^a R_1 = \sum||F_o| - |F_c||/\sum|F_o|$. $^b R_2 = \{\sum[w(F_o^2 - F_c^2)^2]/\sum[w(F_o^2)^2]\}^{1/2}$.

temperature. All absorption corrections were performed using the *SADABS* program. The structure were solved by direct methods and refined by full-matrix least squares on $F^2$ with the *SHELXTL-97* program. The H atoms of organic ligands were geometrically placed and refined using a riding model. However, the H atoms of water molecules in **1** and **2** have not been included in the final refinement. All non-H atoms, except $ClO_4^-$ in **1** and **2**, were refined anisotropically. Cambridge Crystallographic Data Center publications 624300 (**1**) and 624301 (**2**) contain the crystallographic data in CIF format. Further details for structural **1** and **2** analyses are summarized in Table 1, and selected bond lengths of compounds **1** and **2** are listed in Table 2.

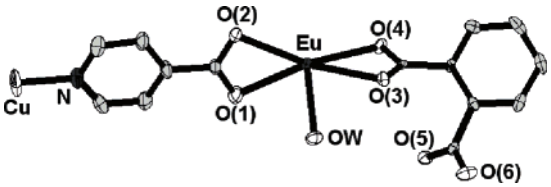


**Figure 2.** Asymmetric unit of **1**. All hydrogen atoms and the $ClO_4^-$ ion are omitted for clarity.

**Table 2.** Selected Bond Lengths (Å) for Compounds **1** and **2**[a]

| | **1** | **2** |
|---|---|---|
| Ln−O(6)#1 | 2.349(11) | 2.346(10) |
| Ln−OW | 2.390(10) | 2.404(9) |
| Ln−O(2) | 2.428(4) | 2.443(5) |
| Ln−O(5) #2 | 2.438(4) | 2.442(4) |
| Ln−O(1) | 2.465(5) | 2.474(5) |
| Ln−O(4)#3 | 2.486(9) | 2.502(8) |
| Ln−O(3) #4 | 2.518(9) | 2.515(8) |
| Ln−O(4) | 2.575(9) | 2.577(8) |
| Ln−O(3) | 2.586(8) | 2.617(8) |
| Cu−N | 1.893(6) | 1.896(7) |
| Cu−N#5 | 1.893(6) | 1.896(7) |

[a] Symmetry codes: #1, $-x + {}^1/_2, y + {}^1/_2, -z$; #2, $x, y, z + 1$; #3, $-x + {}^1/_2, y - {}^1/_2, -z + 1$; #4, $-x + {}^1/_2, y + {}^1/_2, -z + 1$; #5, $-x, y, -z + 2$.

**Scheme 1.** Coordination Mode of the ina (I) and bdc (II) Ligands in **1**

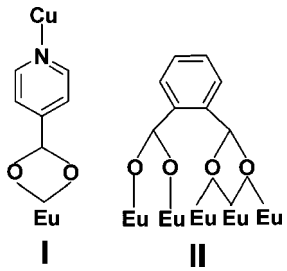


## Results and Discussions

Yellow prism crystals of **1**−**4** were made by the hydrothermal reaction of $Ln_2O_3$, Hina, $H_2bdc$, and $CuCl_2{\cdot}2H_2O$ in water in the presence/absence of $HClO_4$. Compounds **1**−**4** were insoluble in common solvents such as chloroform, toluene, acetonitrile, DMF, methanol, and ethanol. X-ray structure analyses revealed that the frameworks of **1**−**4** are isostructural. Therefore, only the structure of **1** is described in detail. The asymmetric unit of **1** contains one unique $Eu^{3+}$ ion, one $Cu^+$ ion, one ina ligand, and one bdc ligand (Figure 2). The Eu ion is nine-coordinate, and the coordination is close to that of a tricapped trigonal prism or capped square antiprism (Figure S1, Supporting Information): six carboxylate oxygen atoms ($O_{COO}$) from five bdc ligands, two $O_{COO}$ atoms from one bridging ina ligand, and one terminal water molecule. The Eu−O bond lengths vary from from 2.349(11) to 2.586(8) Å (Table 2). Each bdc ligand is coordinated to five $Eu^{3+}$ ions in an unprecedented $\mu_5$-$\kappa^2$,$\kappa^1$,$\kappa^1$,$\kappa^1$,$\kappa^1$ coordination mode and further extended to form the 2D layers (Figure 3a). Although the bdc ligand has more than 15 coordination modes,[10a,12] the mode of II is unique for the bdc ligand (Scheme 1).

The Cu center has a nearly linear coordination environment made up of two N atoms from two bridging ina ligands (Cu−N = 1.893(6) Å, N−Cu−N = 177.7(19)°) (Figure 3b).

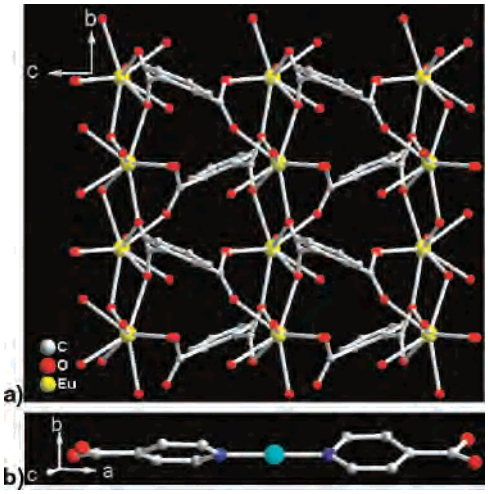


**Figure 3.** View of the individual 2D Ln−bdc network (a) and linear $[Cu(ina)_2]^-$ pillar (b) in **1**. H atoms are omitted for clarity.

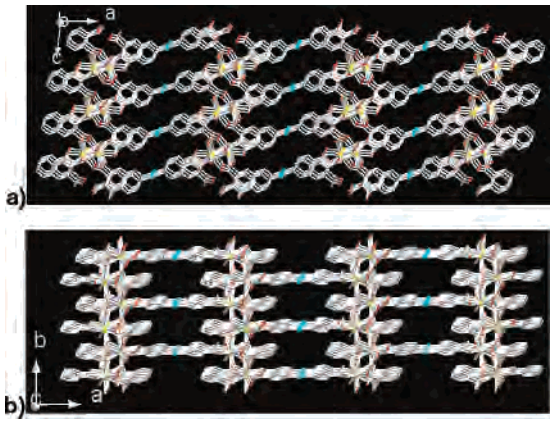


**Figure 4.** Framework of **1** viewed along the *b* (a) and *c* (b) axes, showing two types of channels. All the hydrogen atoms and $ClO_4^-$ ions trapped in the channels are omitted for clarity.

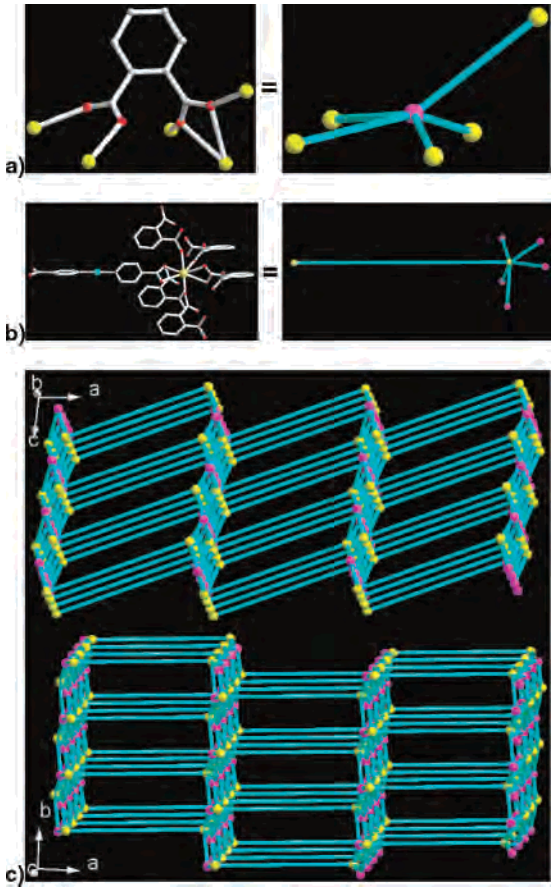


**Figure 5.** (a) bdc ligand regarded as an organic 5-connected node linked with five $Ln^{3+}$ ions (metal nodes, yellow; ligand nodes, purple; similarly represented hereafter). (b) Inorganic 6-connected $Ln^{3+}$ node coordinated with five bdc ligands and one $[Cu(ina)_2]^-$ pillar. (c) Schematic representation of (5,6)-connected net with a unique $(4\cdot7^6 3)(4\cdot7^6 8)$ topology along the *b* and *c* axes.

The isonicotinate ligand binds in a $\mu$-$\kappa^2$O,$\kappa^1$N fashion, chelating $Eu^{3+}$ and bridging $Cu^+$. Although the starting materials are copper(II) salts, the Cu center has an oxidation state of +1, attributed to a reduction reaction involving the ina ligand,[10b,13] which is consistent with a linear geometry for the $Cu^+$ ion.[14] Unless the sheets interpenetrate, the layered structure of the Ln−bdc layer makes it impossible for $Cu^+$ to achieve a higher coordination number, which leads to the unusual linear N−Cu−N mode in $Cu(ina)_2^-$ coordination. The linkages between 2D lanthanide−organic layers and linear $Cu(ina)_2^-$ give rise to a pillared-layer framework having two types of channels along the *b* and *c* axes with dimensions of about 6.2 × 15.8 Å and 7.0 × 8.1 Å (Figure 4), respectively. From the topological point of view, each Eu/bdc layer acts as a six/five-connected node, respectively, and a (5,6)-connected network is formed with the Schläfli symbol of $(4^7\cdot6^3)(4^7\cdot6^8)$ (Figure 5 and Supporting Information Figure S2), which represents a rare example of such net topology.[15] The $ClO_4^-$ groups act as counterions and occupy the void of the interlamellar region to stabilize the lattice. Although the volume of $Cl^-$ is much smaller than that of $ClO_4^-$, the lattice remains stabilized in **4** after the counterion is changed from $ClO_4^-$ to $Cl^-$ if the $HClO_4$ molecule is removed from the reaction,[13] which is further proved by the absence of strong and characteristic Cl−O stretching frequencies around 1090 $cm^{-1}$ in the IR spectrum (Figure S3, Supporting Information).[16]

**IR Spectroscopy.** The IR spectra of **1**−**4** are similar. The strong and broad absorption bands in the range of 3000−3700 $cm^{-1}$ in **1**−**4** are assigned as the characteristic peaks of OH vibration. The strong vibrations appearing around 1590 and 1410 $cm^{-1}$ correspond to the asymmetric and symmetric stretching vibrations of the carboxylate group, respectively. The absence of strong bands ranging from 1690 to 1730 $cm^{-1}$ indicates that the ligands are deproponated, and the strong vibrations appearing around 1090 $cm^{-1}$ in

(12) (a) Cheng, J.-W.; Zhang, J.; Zheng, S.-T.; Zhang, M.-B.; Yang, G.-Y. *Angew. Chem., Int. Ed.* **2006**, *45*, 73. (b) Cañada-Vilalta, C.; Pink, M.; Christou, G. *J. Chem. Soc., Dalton Trans.* **2003**, 1121 and references therein. (c) Song, Y.; Yan, B. *Inorg. Chim. Acta* **2005**, *358*, 191.
(13) Zhang, X.-M. *Coord. Chem. Rev.* **2005**, *249*, 1201.
(14) (a) Yang, W.; Lu, C.; Zhuang, H. *J. Chem. Soc., Dalton Trans.* **2002**, 2879. (b) Lopez, S.; Keller, S. W. *Inorg. Chem.* **1999**, *38*, 1883.
(15) (a) Blatov, V. A.; Carlucci, L.; Ciani, G.; Proserpio, D. M. *CrystEngComm* **2004**, *6*, 377. (b) Delgado-Friedrichs, O.; O'Keeffe, M.; Yaghi, O. M. *Acta Crystallogr., Sect. A* **2006**, *62*, 350.
(16) Wang, R.; Selby, H. D.; Liu, H.; Carducci, M. D.; Jin, T.; Zheng, Z.; Anthis, J. W.; Staples, R. J. *Inorg. Chem.* **2002**, *41*, 278.

**1**−**3** correspond to the the Cl−O stretching frequencies (Figure S3, Supporting Information).

**UV−Vis Spectroscopy.** The diffuse-reflectance UV−vis spectral analyses indicate that **1**−**4** have optical band gaps of 2.34, 2.31, 2.27, and 2.25 eV, respectively. The strong narrow spectral lines in **3** and **4** are attributed to the f−f transitions of $Nd^{3+}$ (Figure S4, Supporting Information).

**Thermal Stability Analyses.** Owing to the similarity of the structures of **1**−**4**, compounds **1**−**2** were selected to examine the thermal stability. The TGA was performed in dry air atmosphere from 30 to 900 °C. These two compounds show similar thermal behavior and undergo two steps of weight loss. The $ClO_4^-$ guest molecules and coordinated water molecules were gradually lost in the temperature range of 70−300 °C for **1** (calcd/found: 12.6/12.0%) and for **2** (calcd/found: 12.6/12.0%). Then the ligands started to decompose, and the residue had a composition of $Eu_2O_3$·CuO for **1** (calcd/found: 40.1/39.6%) and $Sm_2O_3$·CuO for **2** (calcd/found: 39.9/39.1%) (Figure S5, Supporting Information).

**Luminescent Properties.** The solid-state luminescent properties of **1**−**4** were investigated at room temperature. The excitation wavelengths were selected as the maximum of the solid-state excitation spectra (Figure S6, Supporting Information). Complex **1** displays intense red luminescence (Figure 6a) and exhibits the characteristic transition of the $Eu^{3+}$ ion with a decay lifetime of 256.5 $\mu$s; the peaks at 579, 592, 614, 651, and 696 nm are attributed to the $^5D_0 \rightarrow {}^7F_J$ ($J = 0-4$) transitions, respectively. The appearance of the symmetry-forbidden emission $^5D_0 \rightarrow {}^7F_0$ at 579 nm indicates that $Eu^{3+}$ ions in **1** occupy sites with low symmetry and have no inversion center,[17] which is further confirmed by the intensity ratio of about 4.2 for $I(^5D_0 \rightarrow {}^7F_2)/I(^5D_0 \rightarrow {}^7F_1)$; this is in agreement with the result of the single-crystal X-ray analysis. Complex **2** yields red luminescence (Figures 6b) with a decay lifetime of 3.88 $\mu$s when excited at 288 nm; the emissions at 562, 596, and 642 nm are attributed to the characteristic emissions of $^4G_{5/2} \rightarrow {}^6H_J$ ($J = 5/2$, 7/2, and 9/2) transitions of the $Sm^{3+}$ ion. The apparent high intensity of the red luminescence might be derived from the sensitization of the bound ligands to the absence of the ligand-based emission in the fluorescence spectra.

Under excitation at 585 nm, compounds **3** and **4** display three sets of emission bands characteristic of the $Nd^{3+}$ ion in the near-IR region: a strongest emission band at 1064 nm ($^4F_{3/2} \rightarrow {}^4I_{11/2}$), an emission band at 894 nm ($^4F_{3/2} \rightarrow {}^4I_{9/2}$) with a much lower intensity, and a very weak band at 1345 nm ($^4F_{3/2} \rightarrow {}^4I_{13/2}$) (Figure 6c). The profiles of the emission bands for **3** and **4** are in agreement with the previously reported spectra of $Nd^{3+}$ complexes.[18]

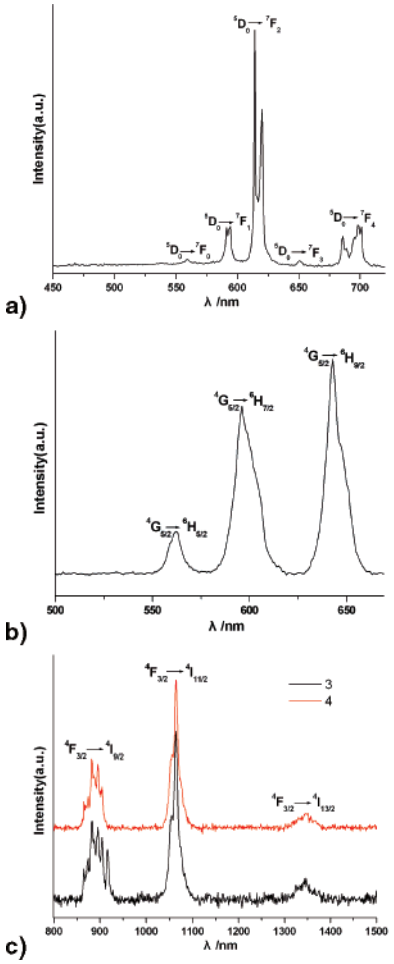


**Figure 6.** Emission spectra of **1** (a) and **2** (b) excited at 288 nm and **3** and **4** (c) excited at 585 nm in the solid state at room temperature.

## Conclusion

In summary, we have successfully synthesized four novel 3D Ln−TM coordination polymers, each with a pillared-layer open framework constructed from lanthanide−organic sheets pillared by linear-coordinated TM. The key point of the synthetic procedures has been well-established. Optical and luminescent properties for **1** and **4** have also been investigated. To the best of our knowledge, this is the first such pillared-layer 3d−4f framework. This work opens new perspectives and a feasible synthetic strategy for the construction of such pillared-layer 3d−4f MOFs; work is continuing in this area.

**Acknowledgment.** This work was supported by the National Natural Science Fund for Distinguished Young Scholars of China (No. 20725101), the 973 Program (No. 2006CB932904), the NNSF of China (No. 20473093), and the NSF of Fujian Province (Nos. E0510030/2005HZ01-1).

**Supporting Information Available:** X-ray crystallographic files in CIF format for structures **1** and **2**, IR spectra, UV−vis spectral data, TGA curves, and additional figures. This material is available free of charge via the Internet at http://pubs.acs.org.

IC700893W

(17) (a) Bünzli, J. C. G.; Piguet, C. *Chem. Soc. Rev.* **2005**, *34*, 1048. (b) Sun, Y.-Q.; Zhang, J.; Chen, Y.-M.; Yang, G.-Y. *Angew. Chem., Int. Ed.* **2005**, *44*, 5814. (c) Sun, Y.-Q.; Zhang, J.; Yang, G.-Y. *Chem. Commun.* **2006**, 1947. (d) Sun, Y.-Q.; Zhang, J.; Yang, G.-Y. *Chem. Commun.* **2006**, 4700.

(18) (a) Yang, J.; Yue, Q.; Li, G.; Cao, J.; Li, G.; Chen, J. *Inorg. Chem.* **2006**, *45*, 2857. (b) Song, J.; Mao, J. *Chem.—Eur. J.* **2005**, *11*, 1417. (c) Cheng, J.-W.; Zheng, S.-T.; Yang, G.-Y. *Dalton Trans.* **2007**, 4059.